PHYSICAL REVIEW B **93**, 140201(R) (2016)

Size effects on the thermal conductivity of amorphous silicon thin films

Jeffrey L. Braun,[1] Christopher H. Baker,[1] Ashutosh Giri,[1] Mirza Elahi,[2] Kateryna Artyushkova,[3] Thomas E. Beechem,[4] Pamela M. Norris,[1] Zayd C. Leseman,[5] John T. Gaskins,[1] and Patrick E. Hopkins[1,*]

[1]*Department of Mechanical and Aerospace Engineering, University of Virginia, Charlottesville, Virginia 22904, USA*

[2]*Department of Electrical and Computer Engineering, University of New Mexico, Albuquerque, New Mexico 87131, USA*

[3]*Department of Chemical and Nuclear Engineering, University of New Mexico, Albuquerque, New Mexico 87131, USA*

[4]*Sandia National Laboratories, Albuquerque, New Mexico 87123, USA*

[5]*Department of Mechanical Engineering and Manufacturing Training and Technology Center, University of New Mexico, Albuquerque, New Mexico 87131, USA*

(Received 6 August 2015; revised manuscript received 5 October 2015; published 1 April 2016)

We investigate thickness-limited size effects on the thermal conductivity of amorphous silicon thin films ranging from 3 to 1636 nm grown via sputter deposition. While exhibiting a constant value up to ∼100 nm, the thermal conductivity increases with film thickness thereafter. The thickness dependence we demonstrate is ascribed to boundary scattering of long wavelength vibrations and an interplay between the energy transfer associated with propagating modes (propagons) and nonpropagating modes (diffusons). A crossover from propagon to diffuson modes is deduced to occur at a frequency of ∼1.8 THz via simple analytical arguments. These results provide empirical evidence of size effects on the thermal conductivity of amorphous silicon and systematic experimental insight into the nature of vibrational thermal transport in amorphous solids.

DOI: 10.1103/PhysRevB.93.140201

The influence of size effects on the phonon thermal conductivity of crystalline thin films has been the topic of a wide array of studies [1–4] that have shaped the direction of fields rooted in nanoscale heat transfer and applications reliant on nanotechnology. It is well known that for films with thicknesses less than the length scale of their phonon mean free paths, thermal conductivity can be reduced due to incoherent boundary scattering of phonons ballistically traversing the film. By comparison, the role of size effects on the thermal conductivity of disordered or fully amorphous solids has been examined to a lesser extent. Unlike crystalline solids, in which a well defined spectrum of phonons exists in a periodically repeating lattice, the vibrational modes in disordered solids are described using a different taxonomy due to the lack of atomic periodicity [5]. In these systems, the vibrational modes can be classified as propagating, delocalized (phononlike) modes called "propagons"; nonpropagating, delocalized modes called "diffusons"; and nonpropagating, localized modes called "locons" [5–8]. Previous studies have demonstrated that propagating modes in disordered and amorphous systems can contribute significantly to the thermal conductivity of certain materials, such as amorphous silicon nitride [9], and disordered silicon-germanium alloys [10,11]. This implies that in highly disordered or amorphous thin films, size effects in the vibrational thermal conductivity can exist depending on the degree to which propagating modes contribute to the thermal conductivity. However, in other amorphous thin films, namely, SiO_2 and Al_2O_3, size effects in the thermal conductivity have not been observed [6,12].

Taken together, the impact of size effects on the thermal conductivity in amorphous solids remains underdeveloped. The study of heat carrier mean free path contributions to thermal conductivity has evolved significantly over the past decade [13] through analytical methods such as the thermal conductivity accumulation function [14] and experimental methods such as time domain thermoreflectance (TDTR) [15] and broadband frequency domain thermoreflectance [16]. In the approach taken here, we use TDTR to measure the thermal conductivity of amorphous silicon films of varying thicknesses, an approach that Zhang *et al.* [4] analytically demonstrated can provide information regarding the spectral dependence of the phonon thermal conductivity in nanosystems. While our results provide similar insight into the role of long mean free path propagons to the thermal conductivity of amorphous silicon as that reported by Liu *et al.* [17], our approach is fundamentally different. The approach of Liu *et al.* relied on varying the modulation frequency, and hence the thermal penetration depth and resulting measurement volume beneath the surface in order to isolate the role of propagons with mean free paths larger than the measurement volume on the thermal conductivity measurement. Our approach of varying the amorphous silicon film thickness in a regime in which we sample a substantial portion of the thickness leads our measurements to be independent of modulation frequency. This allows us to report an intrinsic value of thermal conductivity of our samples, gives direct insight into the role of boundary scattering of propagons on the thermal conductivity in the amorphous silicon, and avoids any potential complications or misconceptions regarding the interpretation of modulation frequency-dependent TDTR data that otherwise could cloud our results [16,18–20].

Examining the vibrational taxonomy discussed above, if the amorphous solid's thermal conductivity contains a significant contribution from propagons compared to nonpropagating modes, then size effects should play a role in thermal conduction. That is, increasing film thickness will reduce propagon-boundary scattering as films approach the length scales of propagon mean free paths, allowing these propagons to contribute to thermal conductivity. Amorphous silicon (a-Si) serves as a suitable candidate to study this hypothesis given the well established literature both experimentally [16,17,21–27]

*phopkins@virginia.edu

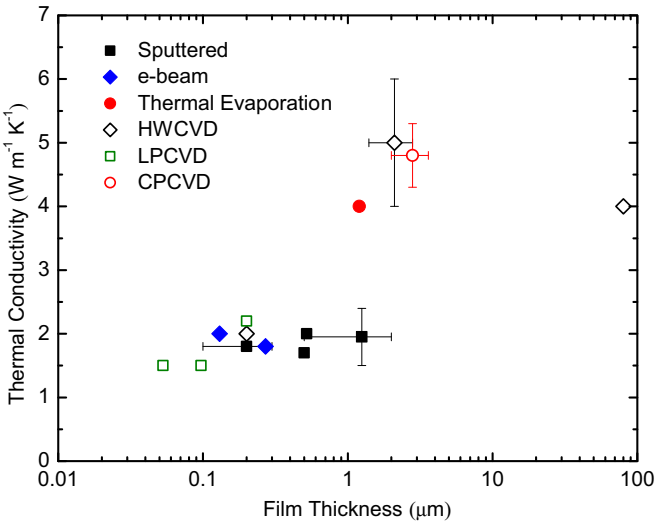

FIG. 1. Literature data for thermal conductivity of amorphous silicon as a function of film thickness: solid squares represent samples prepared via sputter deposition [16,22–24], solid diamonds represent samples prepared via e-beam evaporation [26], open diamonds represent samples prepared via hot-wire chemical vapor deposition (HWCVD) [17,27], open squares represent sample prepared via low-pressure chemical vapor deposition (LPCVD) [25], and closed and open circles represent samples prepared via thermal evaporation and cyclic plasma chemical vapor deposition (CPCVD), respectively [21].

and computationally [5,6,28]. These computational studies suggest that propagons can contribute significantly to thermal conductivity when not restricted by forced scattering (e.g., by boundaries). Thus, clear size effects on the measured thermal conductivity of a-Si films should be observable, driven by propagon-boundary scattering. Figure 1 summarizes the literature data on experimentally measured values of a-Si thermal conductivity as a function of film thickness. While a general trend of increasing thermal conductivity with film thickness is observed, the lack of uniform growth conditions among samples hinders any insight into discerning intrinsic properties from by-products of fabrication or measurement technique. It is clear that in order to study the nature of long-wavelength heat carriers and the role of film thickness on a-Si thermal conductivity, a systematic study with samples prepared under identical growth conditions is necessary.

To this end, we measure the thermal conductivity of a series of amorphous silicon thin films ranging in thickness from 3 to 1636 nm. Our results not only demonstrate size effects in the thermal conductivity, which remain pronounced up to the thickest films, but also show evidence of a crossover from a constant thermal conductivity to an increasing thermal conductivity. We analytically study this trend under the hypothesis that it is driven by an increasing contribution from propagons with increasing a-Si thickness [6]. Using a kinetic theory approach to modeling the thickness-dependent thermal conductivity, we empirically determine a propagon/diffuson crossover frequency in our a-Si samples, which is in excellent agreement with previous theory and molecular dynamic simulations [5,6]. Our results provide experimental support to the progagon/diffuson/locon taxonomy describing the underlying vibrational thermophysics driving the thermal conductivity of a-Si, while also highlighting the shortcomings of the minimum thermal conductivity model for describing the thermal conductivity of thick a-Si films [29].

We fabricated a-Si films on native oxide/silicon substrates using rf sputter deposition. Nominally 80 (±3) nm of Al was deposited on top of the a-Si samples by electron-beam evaporation to act as an optothermal transducer during our thermal conductivity measurements; we verified the thickness of the Al film on each sample using mechanical profilometry and picosecond acoustics [30,31]. As detailed in the Supplemental Material [32], we characterize the a-Si films with x-ray photoemission spectroscopy to quantify the chemical composition and Raman spectroscopy to confirm the amorphous nature of the films.

We measured the thermal conductivity of the a-Si using TDTR, the details and analyses for which are described elsewhere [15,33,34]. Our specific setup is described in Ref. [35]. We measure the ratio of the in-phase to out-of-phase voltage of the probe response as a function of pump-probe delay time using pump and probe $1/e^2$ spot sizes (diameters) of 55 and 13 μm, respectively, while the pump pulses are modulated with an $f = 12.2$ MHz sinusoidally varying envelope. Using a multilayer, radially symmetric thermal model [15,34], we fit for the thermal boundary conductance between the Al transducer and the a-Si film ($h_{\mathrm{K,Al/a\text{-}Si}}$) and the a-Si thermal conductivity ($\kappa_{\mathrm{a\text{-}Si}}$). We assume bulk values for the heat capacity of the Al transducer, a-Si film, and Si substrate [36,37]. Using a modulation frequency of 12.2 MHz, the thermal penetration depth is relatively shallow (roughly 140–180 nm using a calculation for thermal penetration depth as $\delta \approx \sqrt{\kappa_{\mathrm{a\text{-}Si}}/\pi f C_{\mathrm{a\text{-}Si}}}$, where C is the volumetric heat capacity). As a result, for the samples greater than δ, we can measure $h_{\mathrm{K,Al/a\text{-}Si}}$ and $\kappa_{\mathrm{a\text{-}Si}}$ without knowledge of the thermal boundary conductance across the a-Si/native oxide/Si substate interface, and for thicknesses greater than approximately $\delta/0.47$, we can assume the a-Si film as semi-infinite compared to the modulated pump-induced thermal wave [38]. While this semi-infinite assumption simplifies the analysis, we note that to ensure our results are independent of thermal penetration depth, we repeat measurements over modulation frequencies ranging from 1.0 to 12.2 MHz (corresponding to thermal penetration depths between ~150 and 600 nm) and confirm consistency among results [32].

It is important to realize that as the film thickness decreases to thicknesses less than the Al transducer thickness, TDTR measurements become more sensitive to the thermal conductance of the film ($\kappa_{\mathrm{a\text{-}Si}}/d$), where d is the film thickness, and lose sensitivity to the thermal mass of the film (Cd). In this thin-film regime, the intrinsic thermal conduction of the film must be separated from the thermal boundary conductance across the a-Si/native oxide/Si interface ($h_{\mathrm{K,a\text{-}Si/c\text{-}Si}}$), especially when $h_{\mathrm{K,a\text{-}Si/c\text{-}Si}} \approx \kappa_{\mathrm{a\text{-}Si}}/d$ and the thermal penetration depth during TDTR experiments is on the order of, or greater than, the film thickness. In general, this thin-film regime can be loosely defined as having a thickness less than the thermal penetration depth. To appropriately quantify this regime, we apply sensitivity analyses in which we perturb several parameters in our TDTR analysis to determine the magnitude of influence for these parameters on the results [32]. We find that the thermal conductivity measured for samples with

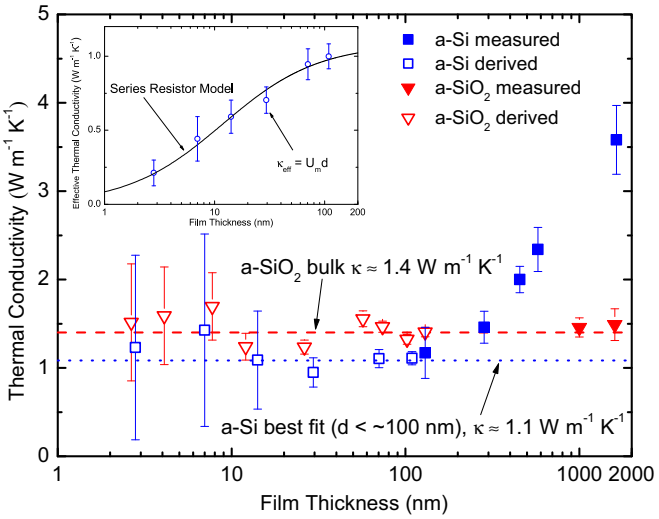

FIG. 2. Thermal conductivity of amorphous silicon (amorphous silica) samples: filled squares (filled triangles) represent thermal conductivity as measured without the influence of $h_{K,a\text{-}Si/c\text{-}Si}$ ($h_{K,a\text{-}SiO_2/Si}$), while open squares (open triangles) denote the derived thermal conductivity as determined using Eq. (2). The dashed line at $\kappa = 1.4$ W m^{-1} K^{-1} represents the literature bulk value of SiO_2 thermal conductivity [40], while the dotted line at $\kappa \approx 1.1$ W m^{-1} K^{-1} represents the fitted value for the thermal conductivity of our a-Si thin films using Eq. (2). Shown in the inset is a plot of effective thermal conductivity of a-Si thin-films vs film thickness and the model using Eq. (2) with best fit values for κ_i and $h_{K,total}$.

thicknesses less than ~150 nm includes an additional thermal resistance due to the substrate interface that masks its intrinsic value.

Analysis of samples within this thin-film regime ($d <$ 150 nm) can be difficult. Lee and Cahill [39] showed that if the intrinsic thermal conductivity is independent of film thickness, a series resistor model can be used to account for the presence of the interface resistance being measured during TDTR. In parallel with molecular dynamics described in detail in the Supplemental Material [32], we systematically study this with the initial assumption that the series resistor model is valid for all film thicknesses in the thin-film regime. To model intrinsic thermal conductivity, we use the following:

$$\frac{1}{U_m} = \frac{1}{h_{K,total}} + \frac{d}{\kappa_i}, \tag{1}$$

where U_m is the total measured thermal conductance across the Al/a-Si interface, a-Si layer, and a-Si/c-Si interface; κ_i is the intrinsic thermal conductivity; and $h_{K,total}$ accounts for the both $h_{K,Al/a\text{-}Si}$ and $h_{K,a\text{-}Si/c\text{-}Si}$ in series using a thermal circuit model. Defining $\kappa_{eff} = U_m d$, we rearrange Eq. (1) to become

$$\kappa_i = \frac{\kappa_{eff}}{1 - \frac{\kappa_{eff}}{h_{K,total} d}}. \tag{2}$$

Using Eq. (2), we fit κ_i and $h_{K,total}$ to our experimental data (six data points classified by the thin-film regime) using a nonlinear least-squares fit. If the aforementioned assumptions are correct, we should observe a good fit to our data. Indeed, this is the case, as shown in the inset to Fig. 2. The best fit value for κ_i is 1.1 (±0.15) W m^{-1} K^{-1} while the best fit value for $h_{K,total}$ is 92 (±30) MW m^{-2} K^{-1}, where uncertainty is based on 95% confidence bounds. To further validate these results, we repeat this procedure using all subsets of data points within the set of films used in this initial calculation; we find a remarkable consistency among all combinations, indicating that this procedure gives an acceptable average for the thermal conductivity for films in the thin-film regime. Moreover, it demonstrates that any film size effects on thermal conductivity are relatively insignificant, such that we proceed under the assumption that thermal conductivity for films less than ~100 nm is constant.

To understand the sensitivity of this data to the fitted value for $h_{K,total}$, we use this value [92 (±30 MW m^{-2} K^{-1}] and corresponding uncertainty to calculate κ_i values for each film thickness via Eq. (2); we denote these values as "derived" thermal conductivities to distinguish them from measured values. Both derived and measured thermal conductivity values are shown as a function of thickness in Fig. 2. Uncertainty in the data includes contribution from uncertainty in Al and a-Si film thickness as well as uncertainty in fitting. Sensitivity to $h_{K,total}$ becomes more prominent with decreasing film thickness, hence the large uncertainty associated with the estimated thermal conductivity of the thinnest films. Note that the 150 nm film, not analyzed with this thin-film procedure, still shows near-negligible film size dependence on its thermal conductivity.

To confirm the validity of this analysis technique, we follow the same procedure with a-SiO_2 thin films grown via dry oxidation. We find that the best fit value for κ_i is ~1.4 (±0.13) W m^{-1} K^{-1}, while the best fit value for $h_{K,total}$ is ~180 (±55) MW m^{-2} K^{-1}, where again uncertainties are based on 95% confidence bounds. This fitted value of 1.4 W m^{-1} K^{-1} is in excellent agreement with the bulk value for thermal conductivity of amorphous silica [40]. Moreover, these findings suggest that any size dependence observed in our a-Si data are not a result of partial oxidation of the films.

We move forward in our analysis with the assertion that the intrinsic thermal conductivity of our a-Si films below ~100 nm is relatively constant ($\kappa_i = 1.1$ W m^{-1} K^{-1}). Figure 2 depicts the thermal conductivity over the entire range of thicknesses measured in this study; a clear increasing thermal conductivity trend is observed with increasing film thickness beyond ~100 nm. Given that the thermal conductivity of these films is determined to be intrinsic to the a-Si layer and that films with thicknesses greater than the thermal penetration depth have near-negligible sensitivity to the a-Si/substrate interface, we hypothesize that our measurements are sensitive to the increasing thermal effusivity of the a-Si due to the increased contribution of propagon modes to thermal transport. In other words, for films with thicknesses less than the mean free path of propagons, these propagons are traversing the thickness of the a-Si ballistically and scattering at the a-Si/c-Si interface, leading to a reduction in the thermal conductivity. Thus, size effects in these long-wavelength modes become less pronounced as the film thickness is increased, leading to an increase in thermal conductivity, an experimental result that has been demonstrated in crystalline solids [1,2] and disordered alloys [10]. As the limit of this contribution to

thermal conductivity by propagons approaches zero, we are left with only contribution by diffusons; we therefore attribute the constant thermal conductivity we derive above to diffuson thermal conductivity. This experimentally observed conclusion is consistent with Larkin and McGaughey's [6] recent molecular dynamics simulations, which predicted a diffusion thermal conductivity in a-Si of 1.2 ($\pm$0.1) W m^{-1} K^{-1} and attributed size effects in a-Si to be driven by propagon-boundary scattering.

We compare this derived value for diffuson thermal conductivity to the prediction from the minimum thermal conductivity ($\kappa_{\min}$) model, given by Cahill *et al.* [29]. For amorphous silicon, $\kappa_{\min}$ as calculated by this model is $\sim$1 W m^{-1} K^{-1}, in close agreement with what we observe in our results. This model treats atomic vibrations as harmonic oscillators having a single frequency and assumes scattering events necessarily occur at distances equal to the interatomic spacing. This $\kappa_{\min}$ model captures the nature of diffusons given the small length scales over which diffusons transfer energy (<10 nm) [28]. However, the model fails to capture the nature of propagon contribution to thermal conductivity, as evidenced by our data in Fig. 2. Thus, an improved model is needed to describe the thermal conductivity of all heat carriers in a-Si.

Our data suggest two regimes of thermal conductivity in a-Si films: the regime of relatively constant thermal conductivity that is dominated by diffuson transport ($d < 100$ nm, $\kappa_{\text{diffuson}} = 1.1$ W m^{-1} K^{-1}) and a regime of increasing thermal conductivity dominated by propagon transport ($d > 100$ nm). Based on these regimes, the rate of increase in thermal conductivity of films in the "propagon-dominated" regime can be directly linked to the propagon/diffuson crossover frequency, so that the propagon contribution to the thermal conductivity of a-Si can be analytically modeled via

$$\kappa_{\text{propagon}} = \frac{1}{3}\sum_j \int_0^{\omega_{p\to d,j}} \hbar\omega D_j(\omega)\frac{\partial f}{\partial T} v_j^2 \tau_j d\omega, \qquad (3)$$

where j is an index that refers to the polarization (longitudinal or transverse), $\omega_{p\to d}$ is the crossover angular frequency (from propagon regime to diffuson regime), $\hbar$ is the reduced Planck's constant, ω is the propagon angular frequency, D is the propagon density of states, f is the propagon equilibrium distribution function (assumed to be Bose-Einstein distribution), v is the sound speed, and τ is the propagon relaxation time. Due to the long-wavelength nature of propagons, we model the density of states using a Debye model based on the sound speeds and atomic density of a-Si [29]. We also assume that relaxation times of propagons can be modeled similarly to umklapp and impurity scattering of long-wavelength phonons in silicon; we use values for these relaxation times based on a three-phonon scattering model of the form $\tau^{-1} = A\omega^4 + BT\omega^2 \exp(-C/T)$ [41–45]. Fitting to bulk literature thermal conductivity data for crystalline silicon sampled over 100–700 K using a Debye approximation, we find that $A = 1.82 \times 10^{-45}$ s^3, $B = 2.8 \times 10^{-19}$ s K^{-1}, and $C = 182$ K. We include a boundary scattering time for the propagons given by $\tau_b = d/(2v_j)$ [6,46]. Finally, we assume $\omega_{p\to d,T} = \omega_{p\to d,L} v_T/v_L$, where "$L$" and "$T$" denote the longitudinal and transverse propagon modes, respectively.

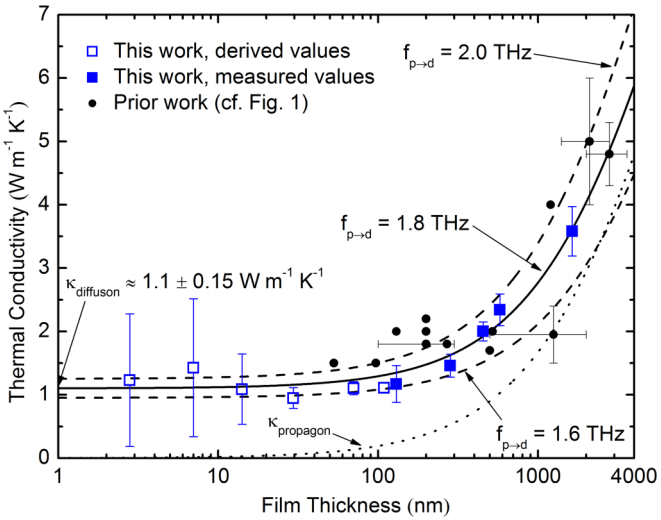

FIG. 3. Thermal conductivity of our a-Si thin films. Open squares denote derived thermal conductivity using Eq. (2), while filled squares denote the thermal conductivity as directly measured. Our thermal conductivity model ($\kappa = \kappa_{\text{diffuson}} + \kappa_{\text{propagon}}$) is plotted with its best fit value for $f_{p\to d}$ of 1.8 THz (solid curve) as well as the individual contribution of κ_{propagon} as calculated using Eq. (3) (dotted curve). Also shown are the calculated curves for the same model using values for $f_{p\to d}$ of 1.6 THz with $\kappa_d = 0.95$ W m^{-1} K^{-1} and 2.0 THz with $\kappa_d = 1.25$ W m^{-1} K^{-1}(dashed curves). Finally, shown in solid circles is the literature data presented in Fig. 1 up to a film thickness of 4 μm to demonstrate agreement between our model and this data.

Figure 3 shows the intrinsic thermal conductivity as a function of film thickness for all a-Si films in this study as well as our model for propagon contribution to thermal conductivity for film thicknesses up to 4 μm. The total thermal conductivity is the sum of thermal conductivity contributions from diffusons (κ_{diffuson}) and propagons (κ_{propagon}). Treating $\omega_{p\to d}$ as a free parameter, we use a least-squares method to fit this model to our experimental data. The best fit value for this propagon-diffuson crossover frequency, $f_{p\to d} = \omega_{p\to d,L}/2\pi$ is $\sim$1.82 ($\pm$0.2) THz, indicating that vibrational frequencies describing a-Si's dispersion relation beyond this value do not behave as propagons. We note the sensitivity of this curve to the fitting parameter; while negligible at smaller film thicknesses, choice of $\omega_{p\to d}$ becomes significant in the propagon-dominated, large film thickness regime. For comparison, we include the literature values of a-Si thermal conductivity as a function of film thickness first presented in Fig. 1. Although simple, our model aligns with both our experimental observations and literature data up to 4 μm. Additionally, our propagon-diffuson crossover frequency agrees well with our molecular dynamics calculation of 2.0 THz [32] as well as that of Larkin and McGaughey, 1.8 THz [6].

In conclusion, we present evidence for size effects in the measured thermal conductivity of amorphous silicon thin films. We show that this size effect can be attributed to the nature of the long-wavelength vibrations. Based on our experimental observations, only propagons with mean free paths greater than $\sim$100 nm contribute significantly to thermal conductivity. For films with thicknesses less than $\sim$100 nm, the thermal conductivity is dominated by diffusons, which do

not show a significant, observable film size dependence for the films measured in this study.

This work was supported, in part, by the Office of Naval Research (149934-101-GG11900-31345). M.E. and Z.C.L. were supported under an award from the National Science Foundation, Division of CMMI Award No.1056077. Finally, this work was supported by the LDRD program at Sandia National Laboratories (SNL). Sandia National Laboratories is a multiprogram laboratory managed and operated by Sandia Corporation, a wholly owned subsidiary of Lockheed Martin Corporation, for the U.S. DOE National Nuclear Security Administration under Contract No. DE-AC04-94AL85000.

[1] A. M. Marconnet, M. Asheghi, and K. E. Goodson, J. Heat Transfer **135**, 061601 (2013).
[2] G. Chen, *Nanoscale Energy Transport and Conversion: A Parallel Treatment of Electrons, Molecules, Phonons, and Photons* (Oxford University Press, New York, 2005).
[3] D. Li, Y. Wu, P. Kim, L. Shi, P. Yang, and A. Majumdar, Appl. Phys. Lett. **83**, 2934 (2003).
[4] H. Zhang, C. Hua, D. Ding, and A. J. Minnich, Sci. Rep. **5**, 9121 (2015).
[5] P. B. Allen, J. L. Feldman, J. Fabian, and F. Wooten, Philos. Mag. B **79**, 1715 (1999).
[6] J. M. Larkin and A. J. H. McGaughey, Phys. Rev. B **89**, 144303 (2014).
[7] J. L. Feldman, P. B. Allen, and S. R. Bickham, Phys. Rev. B **59**, 3551 (1999).
[8] P. B. Allen and J. L. Feldman, Phys. Rev. B **48**, 12581 (1993).
[9] R. Sultan, A. D. Avery, J. M. Underwood, S. J. Mason, D. Bassett, and B. L. Zink, Phys. Rev. B **87**, 214305 (2013).
[10] R. Cheaito, J. C. Duda, T. E. Beechem, K. Hattar, J. F. Ihlefeld, D. L. Medlin, M. A. Rodriguez, M. J. Campion, E. S. Piekos, and P. E. Hopkins, Phys. Rev. Lett. **109**, 195901 (2012).
[11] Y. K. Koh and D. G. Cahill, Phys. Rev. B **76**, 075207 (2007).
[12] S. Shenogin, A. Bodapati, P. Keblinski, and A. J. H. McGaughey, J. Appl. Phys. **105**, 034906 (2009).
[13] K. T. Regner, J. P. Freedman, and J. A. Malen, Nanoscale Microscale Thermophys. Eng. **19**, 183 (2015).
[14] F. Yang and C. Dames, Phys. Rev. B **87**, 035437 (2013).
[15] D. G. Cahill, Rev. Sci. Instrum. **75**, 5119 (2004).
[16] K. T. Regner, D. P. Sellan, Z. Su, C. H. Amon, A. J. H. McGaughey, and J. A. Malen, Nat. Commun. **4**, 1640 (2013).
[17] X. Liu, J. L. Feldman, D. G. Cahill, R. S. Crandall, N. Bernstein, D. M. Photiadis, M. J. Mehl, and D. A. Papaconstantopoulos, Phys. Rev. Lett. **102**, 035901 (2009).
[18] G. T. Hohensee, R. B. Wilson, and D. G. Cahill, Nat. Commun. **6**, 6578 (2015).
[19] K. T. Regner, L. C. Wei, and J. A. Malen, J. Appl. Phys. **118**, 235101 (2015).
[20] Y. K. Koh, D. G. Cahill, and B. Sun, Phys. Rev. B **90**, 205412 (2014).
[21] L. Wieczorek, H. Goldsmid, and G. Paul, *Thermal Conductivity 20* (Springer, New York, 1989), pp. 235–241.
[22] B. S. W. Kuo, J. C. M. Li, and A. W. Schmid, Appl. Phys. A **55**, 289 (1992).
[23] D. G. Cahill, M. Katiyar, and J. R. Abelson, Phys. Rev. B **50**, 6077 (1994).
[24] H. Wada and T. Kamijoh, Jpn. J. Appl. Phys. **35**, L648 (1996).
[25] S. Moon, M. Hatano, M. Lee, and C. P. Grigoropoulos, Int. J. Heat Mass Transf. **45**, 2439 (2002).
[26] B. L. Zink, R. Pietri, and F. Hellman, Phys. Rev. Lett. **96**, 055902 (2006).
[27] H.-S. Yang, D. G. Cahill, X. Liu, J. L. Feldman, R. S. Crandall, B. A. Sperling, and J. R. Abelson, Phys. Rev. B **81**, 104203 (2010).
[28] Y. He, D. Donadio, and G. Galli, Appl. Phys. Lett. **98**, 144101 (2011).
[29] D. G. Cahill, S. K. Watson, and R. O. Pohl, Phys. Rev. B **46**, 6131 (1992).
[30] C. Thomsen, J. Strait, Z. Vardeny, H. J. Maris, J. Tauc, and J. J. Hauser, Phys. Rev. Lett. **53**, 989 (1984).
[31] C. Thomsen, H. T. Grahn, H. J. Maris, and J. Tauc, Phys. Rev. B **34**, 4129 (1986).
[32] See Supplemental Material at http://link.aps.org/supplemental/10.1103/PhysRevB.93.140201 for experimental details and molecular dynamics work.
[33] A. J. Schmidt, Ann. Rev. Heat Transfer **16**, 159 (2013).
[34] P. E. Hopkins, J. R. Serrano, L. M. Phinney, S. P. Kearney, T. W. Grasser, and C. T. Harris, J. Heat Transfer **132**, 081302 (2010).
[35] R. Cheaito, C. S. Gorham, A. Misra, K. Hattar, and P. E. Hopkins, J. Mater. Res. **30**, 1403 (2015).
[36] Y. S. Touloukian, R. W. Powell, C. Y. Ho, and P. G. Klemens, *Thermophysical Properties of Matter—Specific Heat: Nonmetallic Solids* (IFI/Plenum, New York, 1970), Vol. 5 .
[37] Y. S. Touloukian and E. H. Buyco, *Thermophysical Properties of Matter—Specific Heat: Metallic Elements and Alloys*. (IFI/Plenum, New York, 1970), Vol. 4 .
[38] J. Liu, J. Zhu, M. Tian, X. Gu, A. Schmidt, and R. Yang, Rev. Sci. Instrum. **84**, 034902 (2013).
[39] S.-M. Lee and D. G. Cahill, J. Appl. Phys. **81**, 2590 (1997).
[40] T. Yamane, N. Nagai, S.-i. Katayama, and M. Todoki, J. Appl. Phys. **91**, 9772 (2002).
[41] P. Klemens, in *Proceedings of the Royal Society of London A: Mathematical, Physical and Engineering Sciences* (The Royal Society, London, 1951), Vol. 208, pp. 108–133.
[42] C. Herring, Phys. Rev. **95**, 954 (1954).
[43] J. Callaway, Phys. Rev. **113**, 1046 (1959).
[44] M. G. Holland, Phys. Rev. **132**, 2461 (1963).
[45] G. A. Slack and S. Galginaitis, Phys. Rev. **133**, A253 (1964).
[46] A. J. H. McGaughey, E. S. Landry, D. P. Sellan, and C. H. Amon, Appl. Phys. Lett. **99**, 131904 (2011).